

Experimental and quantum chemical study on the DNA/protein binding, and biological activity of rhodium(III) complex with 1,2,4-triazole as inert ligand

*Angelina Petrović,^a Marko Živanović,^e Ralph Puchta,^{b,c,d} Dušan Čoćić,^a Andreas Scheurer,^b Nevena Milivojevic ^e and Jovana Bogojeski^{*a}*

^a *University of Kragujevac, Faculty of Science, Radoja Domanovića 12, 34000 Kragujevac, Serbia*

^b *Inorganic Chemistry, Department of Chemistry and Pharmacy, University of Erlangen-Nürnberg, 91058 Erlangen, Germany*

^c *Computer Chemistry Center, Department of Chemistry and Pharmacy, University of Erlangen-Nürnberg, 91058 Erlangen, Germany*

^d *ZISC (Zentralinstitut für Scientific Computing), Universität Erlangen-Nürnberg, Martensstrasse 5a, 91058 Erlangen, Germany*

^e *University of Kragujevac, Institute of Information Technologies Kragujevac, Jovana Cvijića bb, 34000 Kragujevac, Serbia*

**Corresponding author:*

Dr. Jovana Bogojeski
Department of Chemistry
Faculty of Science
University of Kragujevac
Radoja Domanovića 12
Tel: +381(0)34336223
Fax: +381 (0)34 335040
e-mail: jovana.bogojeski@pmf.kg.ac.rs

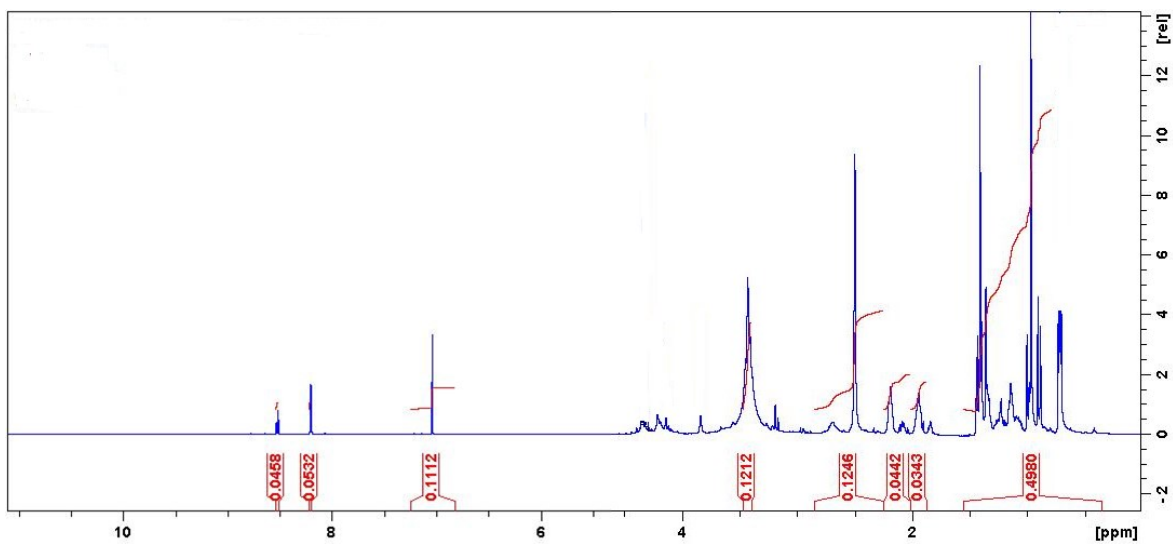


Fig. S1. ¹H NMR spectra of the complex **Rhtrz**

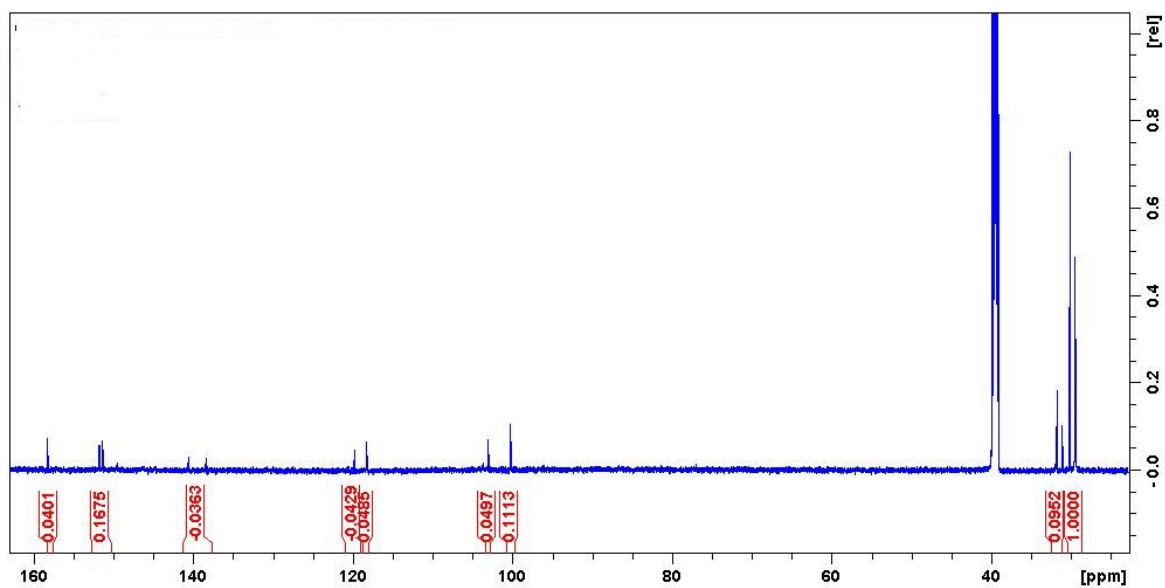


Fig. S2. ¹³C NMR spectra of the **Rhtrz** complex.

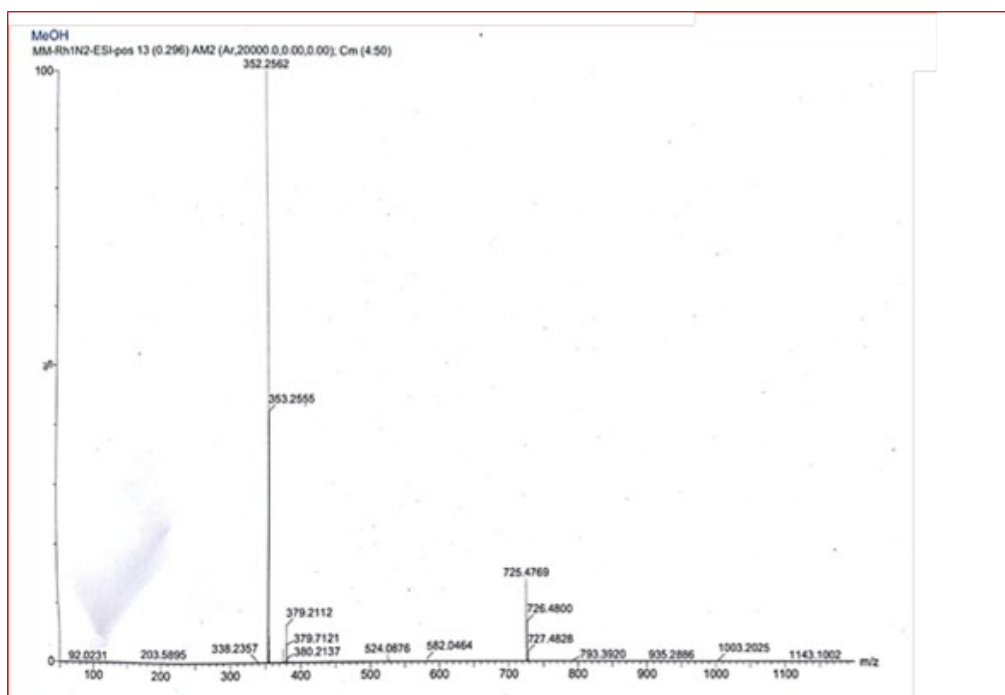


Fig. S3. ESI mass spectra for the **Rhtrz** complex.

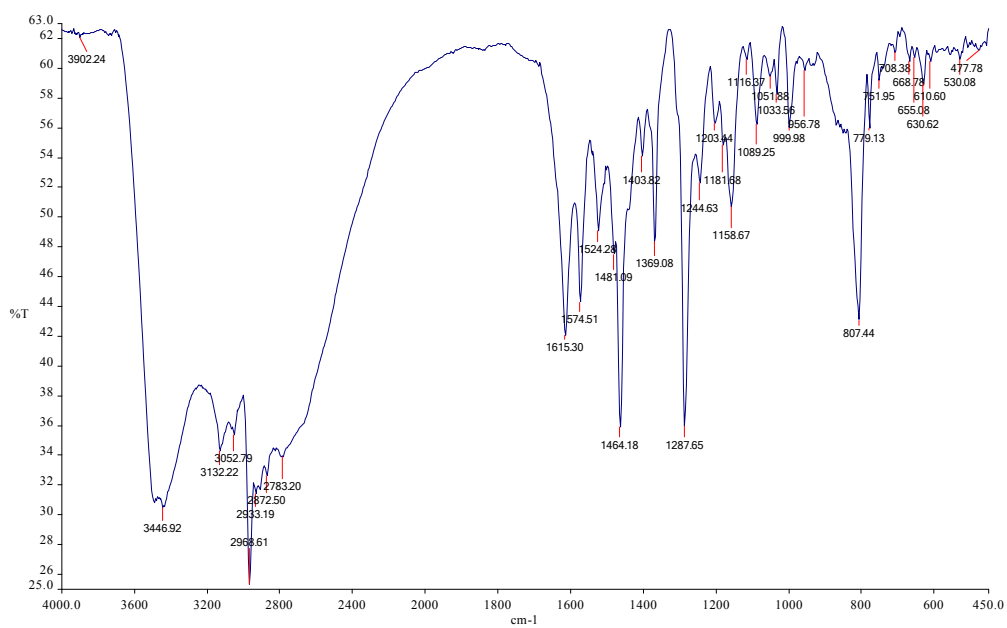


Fig. S4. IR spectra of the **Rhtrz** complex.

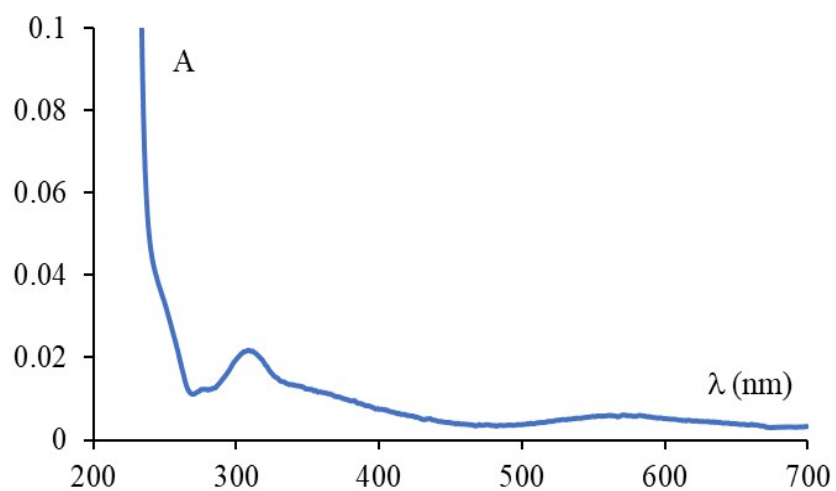


Fig. S5. UV-vis spectra of the **Rhtrz** complex.

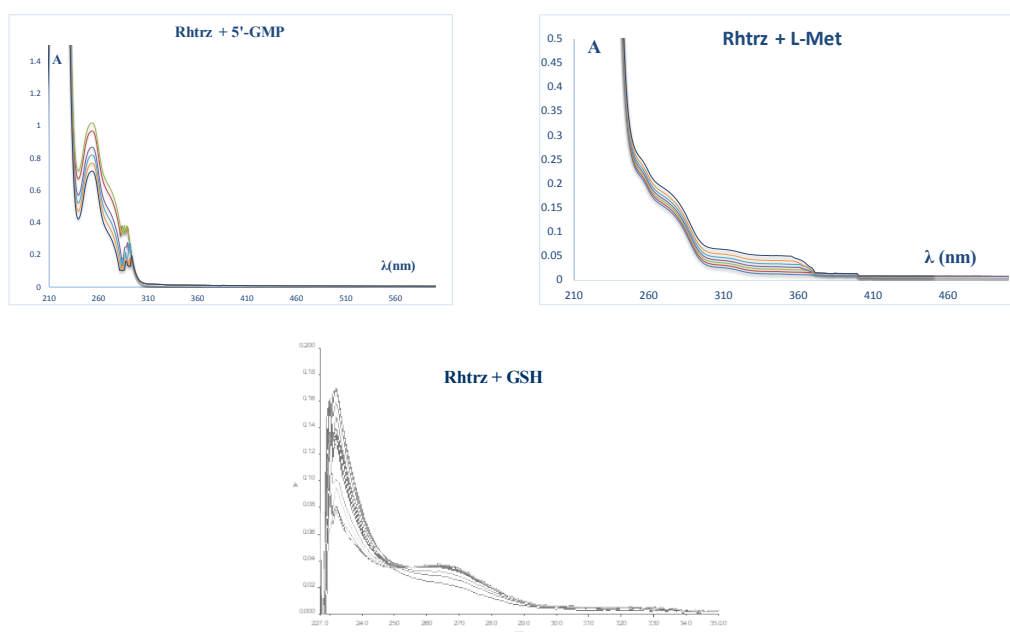


Fig. S6. The change absorbance vs. λ for the substitution reactions of complex Rhtrz with 5'-GMP, L-Met and GSH.

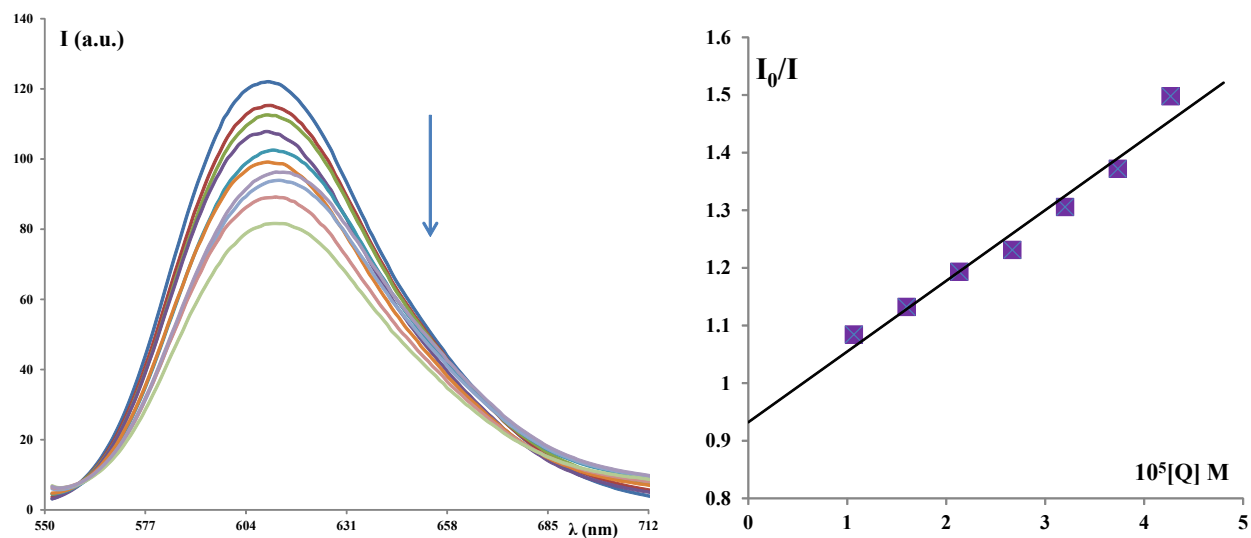


Fig. S7. Emission spectra of EB-DNA in the presence of the **Rhtrz** complex. $[EB] = 10 \mu\text{M}$, $[DNK] = 10 \mu\text{M}$, $[\text{complex}] = 0\text{-}10 \mu\text{M}$; $\lambda_{\text{ex}} = 527 \text{ nm}$. Arrows show changes in intensity after adding solutions of the growing complex concentration; The dependence of I_0/I on the concentration $[Q]$ ($Q = \text{complex}$) where the experimental points are denoted by (■), and the full lines represent the linear dependence.

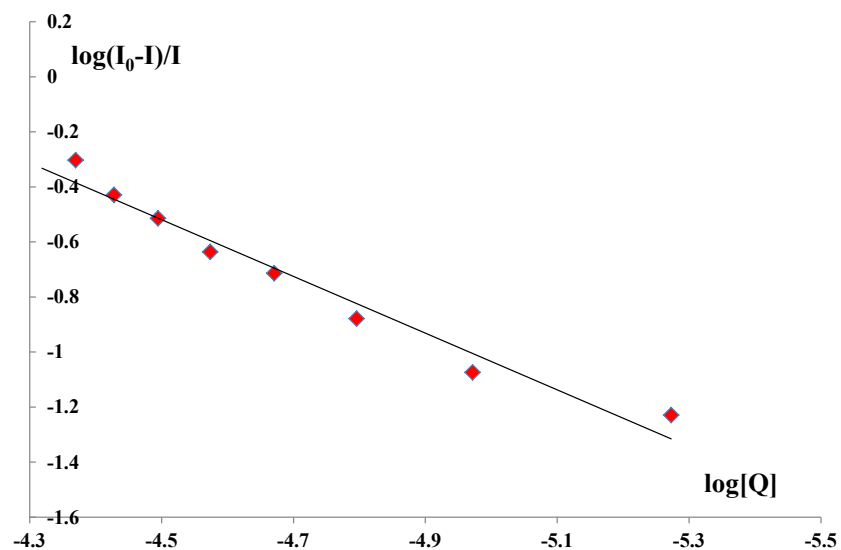


Fig. S8. Dependency $\log [(I_0-I) / I]$ of $\log [Q]$ for the interaction between **Rhtrz** complex and DNA in the presence of EB; $Q = (\text{Complex Rhtrz})$.

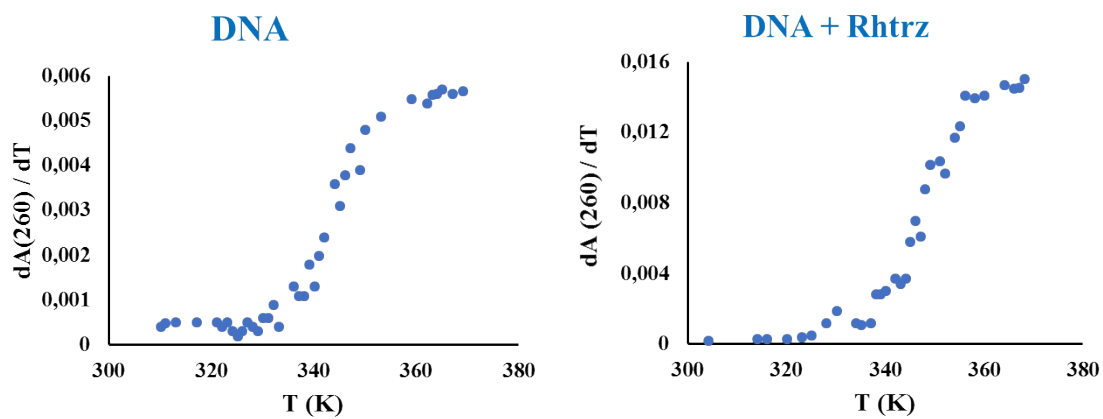


Fig. S9. The derivative plot (dA_{260}/dT vs. T) for DNA in absens and present of **Rhtrz** complex.

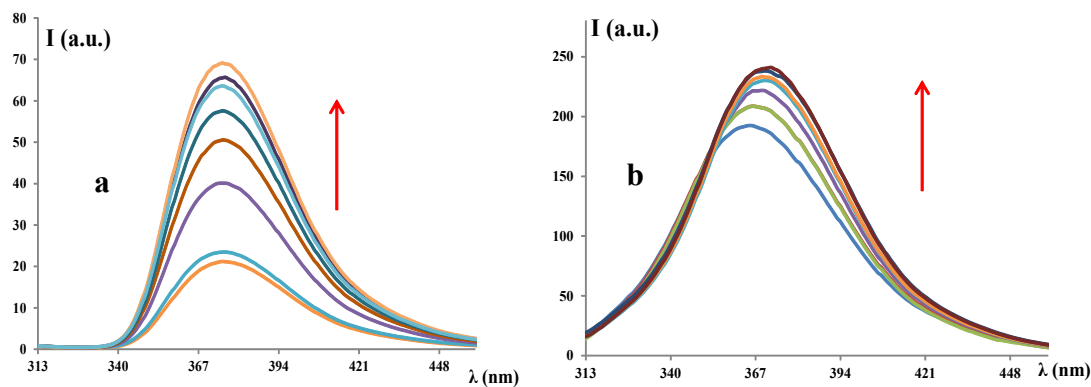


Fig. S10. a) Emission spectra of the complex **Rhtrz**, [complex] = 0-10 μM , λ_{ex} = 295 nm; b) Emission spectra of serum albumin in the presence of the **Rhtrz** complex, [serum albumin] = 2 μM , [complex] = 0-10 μM , λ_{ex} = 295 nm. Arrows show changes in intensity after adding solutions of the growing concentration complex.

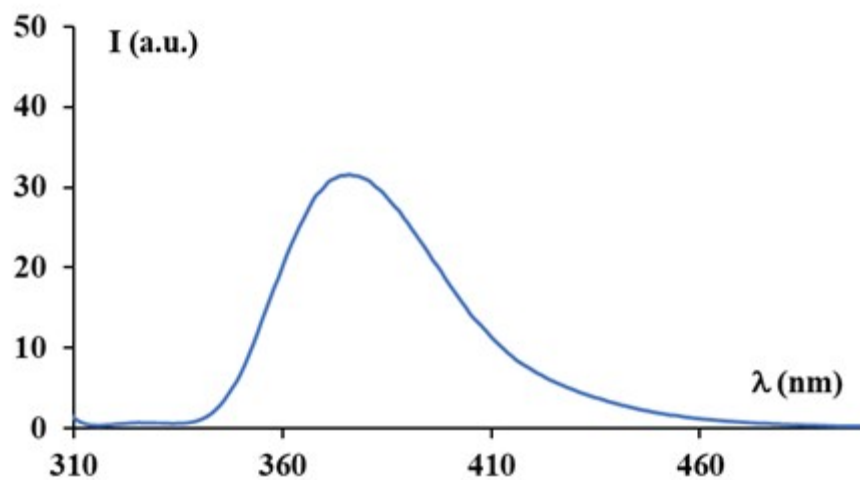


Fig. S11. Fluorescence spectra of the **Rhtrz** complex.

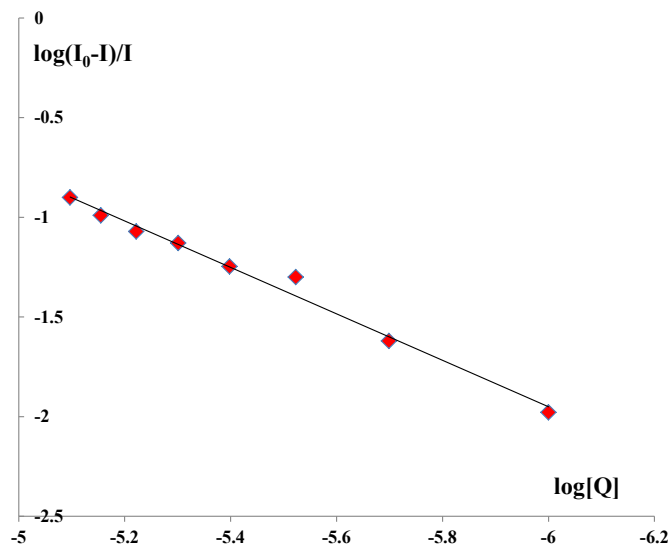


Fig. S12. Log dependency $\log[(I_0-I)/I]$ of $\log[Q]$ for the interaction between **Rhtrz** complex and BSA; $Q = (\text{Complex Rhtrz})$. It can be concluded from the data presented in Table 3. that the investigated **Rhtrz** complex interacts moderately with BSA.

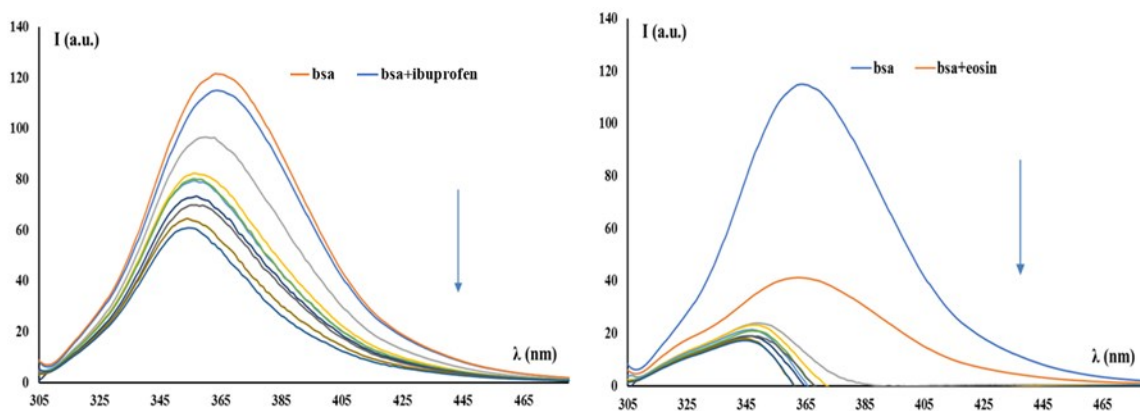


Fig. S13. Fluorescence spectra of BSA, BSA in presence of the site marker with absents and presence of **Rhtrz** complex in rising concertation. Both the concentration of BSA and the site

markers are 2×10^6 mol. The arrow shows the emission intensity changes upon adding correspondent site marker and the increasing the concentration of the **Rhtz** complex.

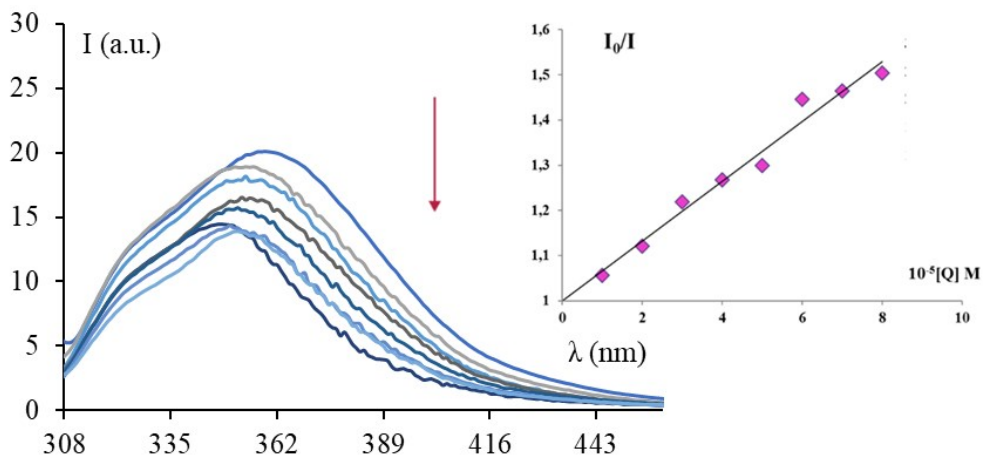


Fig. S14. The dependence of I_0/I on the concentration of $[Q]$ ($Q = \text{complex}$), where the experimental points are denoted by (■), and the full lines represent a linear dependence.

Embedded graph: Emission spectra of serum albumin in the presence of the **Rhtz** complex

$[\text{serum albumin}] = 2 \text{ } \mu\text{M}$, $[\text{complex}] = 0\text{-}10 \text{ } \mu\text{M}$, $\lambda_{\text{ex}} = 280 \text{ nm}$. Arrows show changes in intensity after adding solutions of the growing complex concentration.

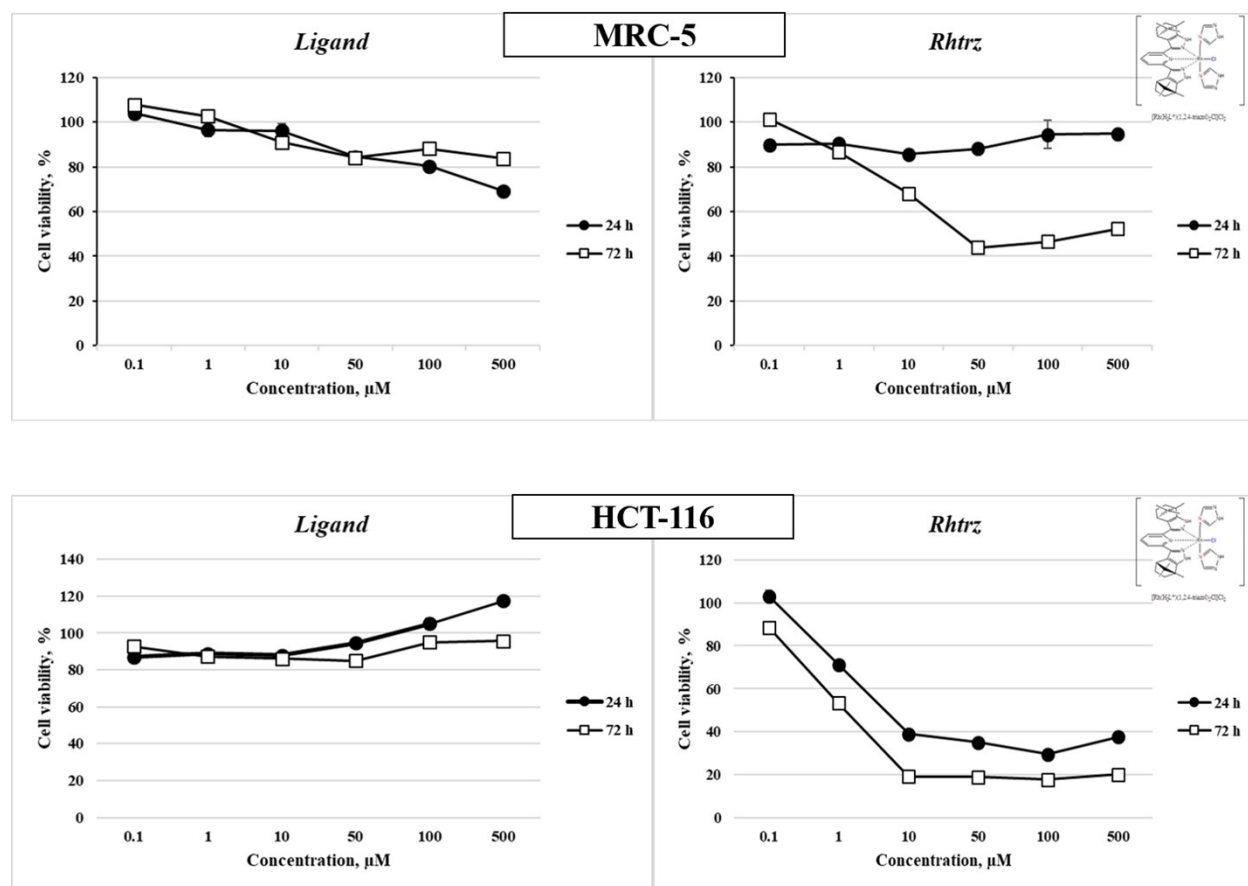


Fig. S15. Cell viability after 24 and 72 h of exposure, expressed in percentages of viable cells.

Brief experimental outline - NBT procedure and Griess protocol.

NBT procedure:

The concentration of superoxide anion radical ($O_2^{\cdot-}$) produced by the cells was determined using a spectrophotometric method based on the reduction of nitroblue tetrazolium (NBT) to nitroblue-formazan in the presence of $O_2^{\cdot-}$. 24h after cell seeding (30.000 per well), the cells were treated with 100 μ l of the tested substances. After another 24h and 72h from treatment, the cells were tested on the production of $O_2^{\cdot-}$.

The assay is performed by a replacement of the DMEM containing substance with 10 μ l of NBT (2.5 mg per mL dissolved in PBS) and the addition of 100 μ l of fresh DMEM. After 3h incubation period at 37 $^{\circ}$ C in 5% CO_2 , the cells have been washed three times with warm PBS and one time with methanol. This washing step is crucial for the removal of the extracellular $O_2^{\cdot-}$. Then, with the addition of 100 μ l 2M KOH, the cells membrane was removed, and formazan crystals have been dissolved in 100 μ l DMSO. After 15 minutes of incubation in the dark, the purple color absorbance was quantified spectrophotometrically on a microplate reader at 550 nm. The amount of reduced NBT was determined by the change in absorbance, based on the molar extinction coefficient for monoformazan that is 15000 $M^{-1} cm^{-1}$, and the results were expressed as μ M.

Griess procedure:

The concentration of nitrites, NO_2^- (an indicator of the NO level) was determined spectrophotometrically using the Griess method [Griess P. *Bemerkungen zu der Abhandlung der HH. Weselky und Benedikt Ueber einige Azoverbindungen. Ber Dtsch Chem Ges* 1879;12:426-428]. Same as in the NBT assay, 30.000 cells were seeded per well and treated with 100 μl of the investigated substances. 24h and 72h from the treatment, the NO_2^- assay was performed. The first step included dislocation of 50 μl of DMEM from each well to another plate. Then, equal volumes of 0.1% (1 mg/ml) N-(1-naphthyl)ethylenediamine and 1% (10 mg/ml) sulfanilic acid (solution in 5% phosphoric acid) were added to form the Griess reagent. After 15 minutes incubation period in the dark at room temperature, the chromophoric azo product that absorbs strongly at 550 nm was recorded using the ELISA reader. The results were expressed in μM NO_2^- from a standard curve established in each test, constituted of known molar concentrations of nitrites.

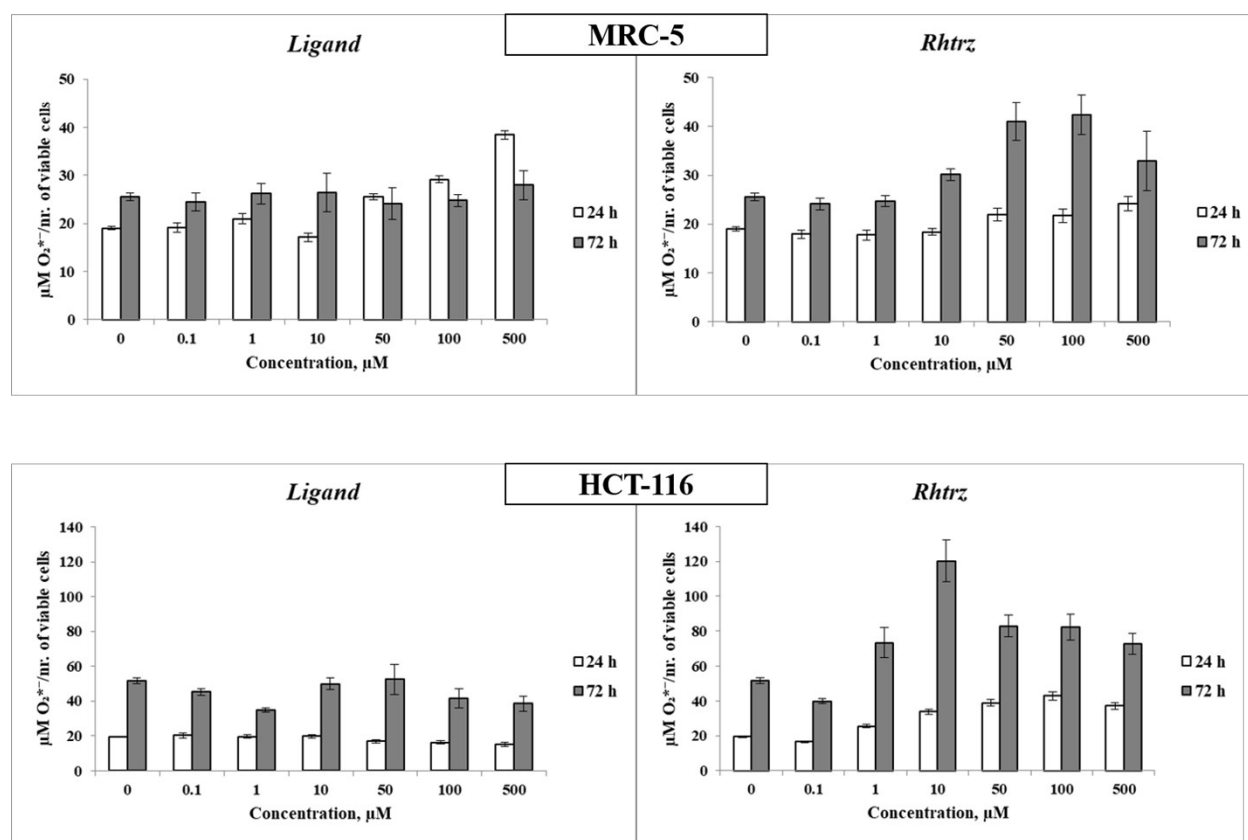


Fig. S16. Effects of ligand and **Rhtrz** complex on MRC-5 and HCT-116 cell lines, expressed as the $\text{O}_2^{\bullet -}$ concentration after 24 h and 72 h of exposure.

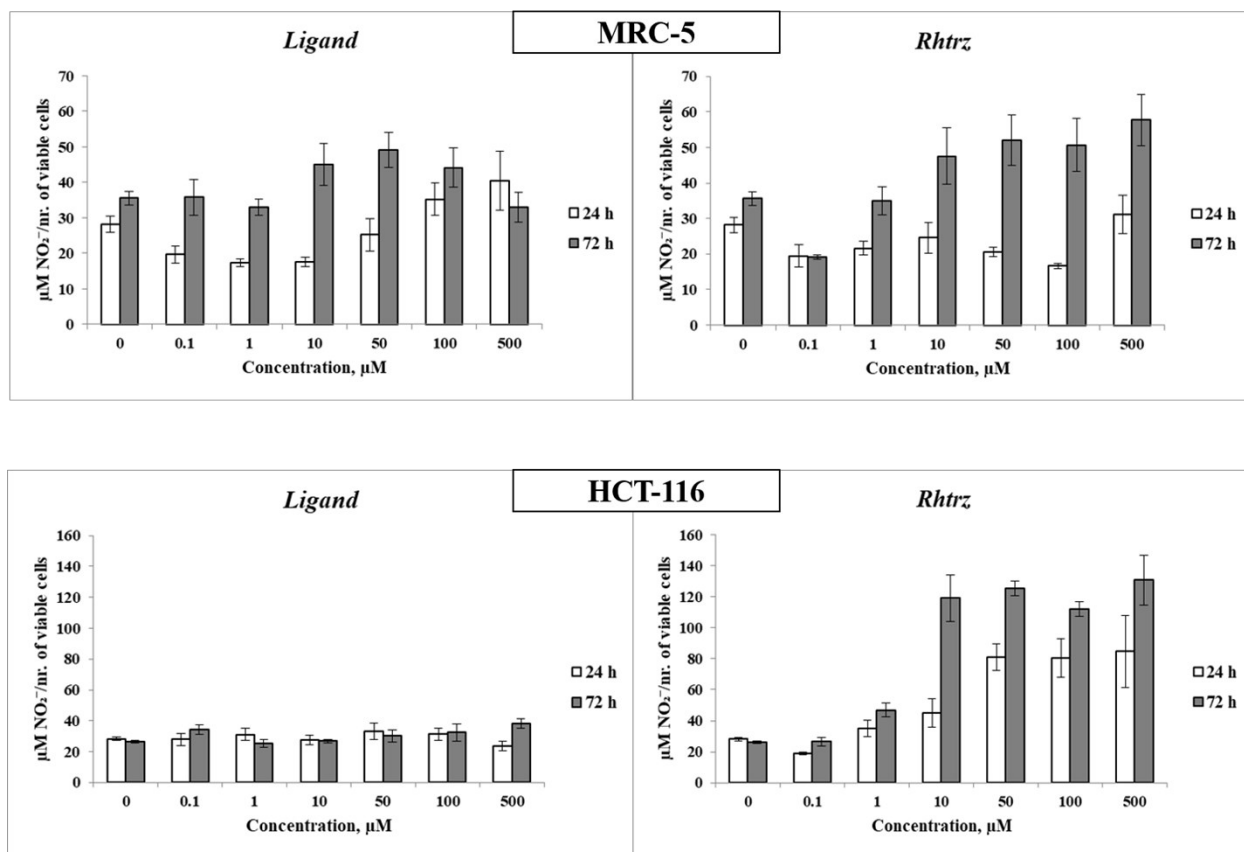


Fig. S17. Effects of ligand and **Rhtrz** complex on MRC-5 and HCT-116 cell lines, expressed as the nitrites concentration after 24 h and 72 h of exposure.

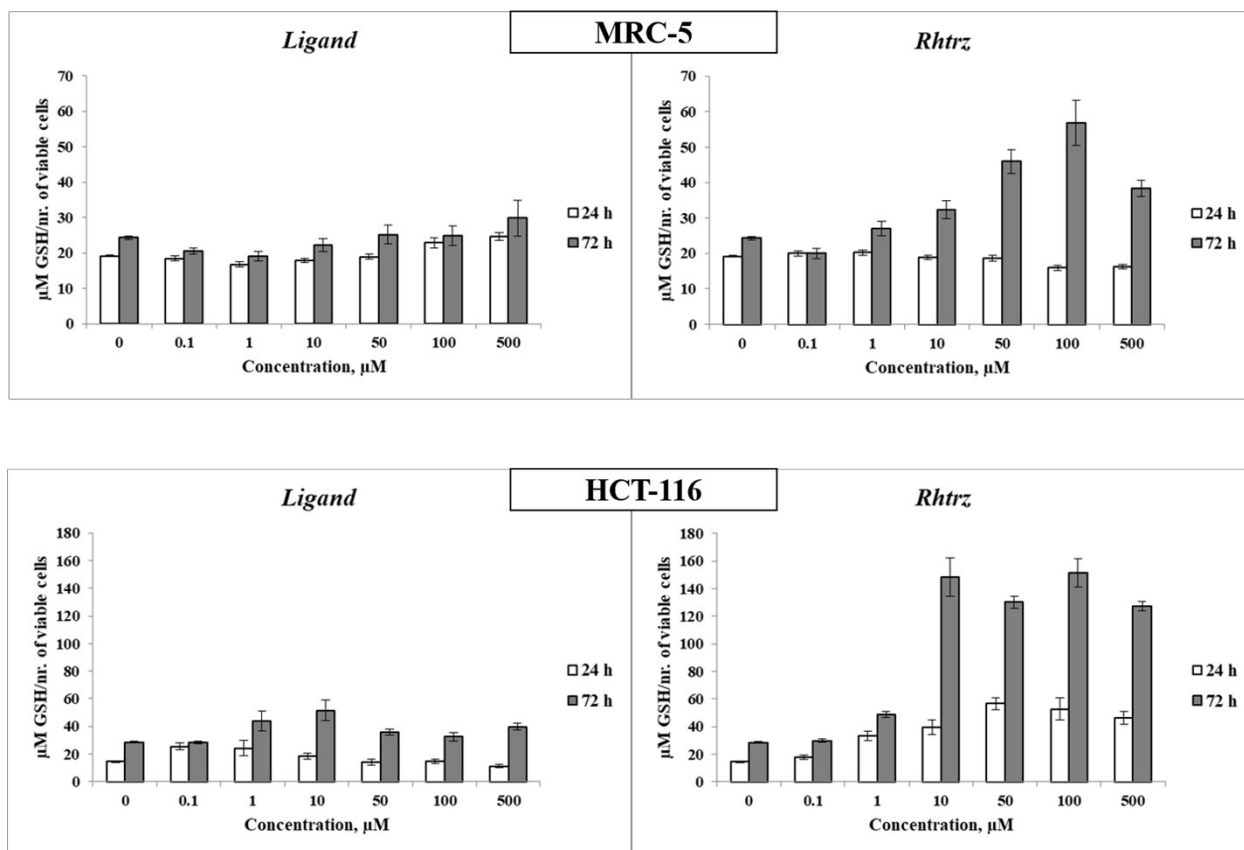


Fig. S18. Effects of ligand and **Rhtrz** complex on MRC-5 and HCT-116 cell lines, expressed as the glutathione concentration after 24 h and 72 h of exposure.

Table S1. Observed *pseudo*-first order rate constants as a function of complex concentration for the reaction between complex **Rhtrz** ($1 \cdot 10^5$ M) and 5'-GMP at pH = 7.2 (25 mM Hepes buffer) in the presence of 30 mM NaCl at 310 K.

T(K)	$10^4 C_{5'-GMP}/M$	k_{obs}/s^{-1}	$C_{complex}/C_{5'-GMP}$
310.0	2.5	/	25
	2.0	0.00016	20
	1.5	0.00014	15
	1.0	0.00012	10
	0.5	0.00011	10*

*Reduced concentration of the complex to $0.5 \cdot 10^5$ M to get another point on the graph, and keep the ratio pseudo-first order.

Table S2. Observed *pseudo*-first order rate constants as a function of complex concentration for the reaction between complex **Rtrz** ($1 \cdot 10^5$ M) and GSH at pH = 7.2 (25 mM Hepes buffer) in the presence of 30 mM NaCl at 310 K.

T(K)	$10^4 C_{(GSH)}/M$	k_{obs}/s^{-1}	$C_{complex}/C_{GSH}$
310.0	2.5	0.0019	25
	2.0	0.0018	20
	1.5	0.0012	15
	1.0	0.0009	10
	0.5	0.0006	10*

*Reduced concentration of the complex to $0.5 \cdot 10^5$ M to get another point on the graph, and keep the ratio pseudo-first order.

Table S3. Observed *pseudo*-first order rate constants as a function of complex concentration for the reaction between complex **Rhtrz** (1×10^5 M) and L-Met at pH = 7.2 (25 mM Hepes buffer) in the presence of 30 mM NaCl at 310, 298 and 288 K.

T(K)	$10^4 C_{\text{L-Met}}/\text{M}$	$k_{\text{obs}}/\text{s}^{-1}$	$C_{\text{complex}}/C_{\text{L-Met}}$
310.0	2.5	0.0014	25
	2.0	0.0012	20
	1.5	0.00098	15
	1.0	0.00057	10
	0.5	0.00040	10*

*Reduced concentration of the complex to 0.5×10^5 M to get another point on the graph, and keep the ratio pseudo-first order.

Table S4. The rate constants for the back-substitution reactions of the Rh^{III} complex with L-Met, 5'-GMP, and GSH at pH = 7.2 (25 mM Hepes buffer) in the presence of 30 mM NaCl.

	5'-GMP $k_1[\text{Cl}^-]$ $\text{M}^{-1}\text{s}^{-1}$	L-Met $10^1 k_1[\text{Cl}^-]$ $\text{M}^{-1}\text{s}^{-1}$	GSH $10^1 k_1[\text{Cl}^-]$ $\text{M}^{-1}\text{s}^{-1}$
Rhtrz	$(9.0 \pm 0.1) 10^{-5}$	/	/